

Impacts of recombination at the surface and in the substrate on carrier lifetimes of n-type 4H–SiC epilayers

Tsunenobu Kimoto,^{1,2,a)} Toru Hiyoshi,¹ Toshihiko Hayashi,¹ and Jun Suda¹

¹*Department of Electronic Science and Engineering, Kyoto University, A1-301, Katsura, Nishikyo, Kyoto 615-8510, Japan*

²*Photonics and Electronics Science and Engineering Center, Kyoto University, Katsura, Nishikyo, Kyoto 615-8510, Japan*

(Received 24 July 2010; accepted 30 August 2010; published online 28 October 2010)

After remarkable reduction in the $Z_{1/2}$ center in n-type 4H–SiC epilayers, the measured carrier lifetimes can be severely affected by other recombination paths. Impacts of carrier recombination at the surface as well as in the substrate are investigated in detail by using numerical simulation based on a diffusion equation. The simulation reveals that a very thick ($>100 \mu\text{m}$) epilayer is required for accurate measurement of carrier lifetimes if the bulk lifetime in the epilayer is longer than several microsecond, due to the extremely short lifetimes in the substrate. The fast decay often observed at the initial stage of decay curves can be explained by fast recombination at the surface and in the substrate. In experiments, the carrier lifetime is improved from 0.69 to 9.5 μs by reducing the $Z_{1/2}$ center via two-step thermal treatment (thermal oxidation and Ar annealing) for a 148- μm -thick n-type epilayer. This lifetime must be still, to large extent, affected by the recombination at the surface and in the substrate, and the real bulk lifetime may be much longer. The carrier recombination paths and their impacts on the decay curves are discussed. © 2010 American Institute of Physics. [doi:10.1063/1.3498818]

I. INTRODUCTION

Silicon carbide (SiC) has received increasing attention as an attractive wide bandgap semiconductor for developing high-power and high-temperature devices.^{1,2} Through recent progress in growth and device processing technology of SiC, high-voltage 4H–SiC Schottky barrier diodes and vertical junction field-effect transistors have been developed.^{3,4} To realize SiC power devices with blocking voltage higher than several kilovolts for very high-voltage applications such as electric power transmission, bipolar devices, such as PiN diodes and thyristors, possess great promise in terms of lower on-resistances owing to the effect of conductivity modulation.^{5,6} Solid state transformers based on 15 kV SiC insulated gate bipolar transistors and 15 kV SiC PiN diodes have been proposed as an attractive application.⁷ In such ultra high-voltage power devices, a long carrier lifetime is required to modulate the conductivity of very thick voltage-blocking layers. For example, a lifetime longer than 5 μs will be required for effective conductivity modulation in 15 kV SiC devices.

The carrier lifetimes in SiC have been intensively investigated by several groups in recent years. Bergman and co-workers have reported a correlation between the lifetime and small-angle grain boundaries,⁸ boron impurity,^{9,10} and a few deep traps.^{10,11} They also reported the improvement of measured carrier lifetimes with increasing the thickness of SiC epilayers.⁸ Tawara *et al.*¹⁴ showed that the $Z_{1/2}$ (Ref. 12) and/or EH6/7 (Ref. 13) centers, which are energetically located at 0.65 eV and 1.55 eV below the conduction band edge, respectively, affect the lifetimes of 4H–SiC epilayers.

More recently, Klein *et al.*¹⁵ and the authors' group¹⁶ have clearly shown that the inverse of the carrier lifetime is proportional to the concentration of the $Z_{1/2}$ center. Based on these results, detailed recombination dynamics via deep levels in 4H–SiC epilayers have been investigated.^{17–19} Now the $Z_{1/2}$ center is well recognized as the dominant lifetime killer, at least, in n-type 4H–SiC,¹⁹ although the microscopic nature is still an open question.^{20–22} It has been also demonstrated that extended defects (dislocations, stacking faults) cause local reduction in carrier lifetimes in SiC epilayers.^{23,24}

In the meantime, successful elimination of the $Z_{1/2}$ center has been achieved by post-growth processes. Tsuchida and co-workers utilized carbon ion implantation followed by high-temperature annealing at 1700–1800 °C to eliminate the $Z_{1/2}$ center below the detection limit ($5 \times 10 \text{ cm}^{-3}$) and demonstrated remarkable improvement of carrier lifetimes.^{25–27} The authors have succeeded in similar elimination of the $Z_{1/2}$ center and lifetime improvement by thermal oxidation.²⁸ Two-step thermal treatment, namely thermal oxidation and inert (Ar) annealing at high temperature, has been proposed for further defect elimination and lifetime improvement.²⁹ After the $Z_{1/2}$ center is significantly reduced by these processes, the carrier lifetimes in 4H–SiC can be limited by other recombination paths. Although the authors suggested the influence of surface and substrate recombination on the carrier lifetime measurements,¹⁸ quantitative analyses are missing. In this study, impacts of recombination at the surface and in the substrate are systematically investigated by using numerical simulation. It is demonstrated that very thick epilayers are required for accurate lifetime measurements. A long carrier lifetime of 9.5 μs at room temperature is experimentally presented, and the recombination paths are discussed.

^{a)}Electronic mail: kimoto@kuee.kyoto-u.ac.jp.

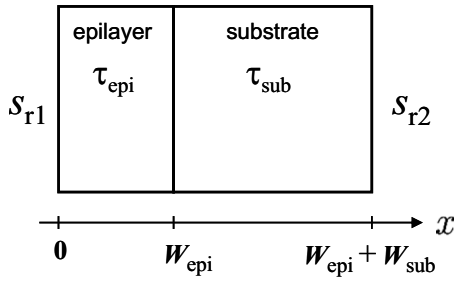


FIG. 1. Schematic illustration of a 4H-SiC epilayer (thickness W_{epi}) grown on a 4H-SiC substrate (thickness: $W_{\text{sub}}=300 \mu\text{m}$). The bulk lifetimes in epilayer and substrate are denoted by τ_{epi} and τ_{sub} , respectively. The bulk lifetime in the substrate (τ_{sub}) was fixed at $0.04 \mu\text{s}$, as experimentally measured. The lifetime, the thickness, and the SRV of the epilayer were varied as parameters.

II. MODEL FOR NUMERICAL SIMULATION OF CARRIER DIFFUSION AND RECOMBINATION

In this study, the depth profile of excess carriers and the decay curves in the lifetime measurements of SiC were analyzed by numerical simulation. The basic equation is the same as that the authors previously reported¹⁸ but the spatial and time resolutions have been improved. The one-dimensional carrier diffusion equation taking account of carrier recombination is given by

$$\frac{\partial p_e}{\partial t} = D \frac{\partial^2 p_e}{\partial x^2} - \frac{p_e}{\tau}. \quad (1)$$

Here the p_e is the concentration of excess holes in the n-type semiconductor, D the diffusion constant, and τ the bulk lifetime. The origin of the x coordinate was taken at the surface of an epilayer.

Figure 1 shows a schematic illustration of a 4H-SiC epilayer (thickness W_{epi}) grown on a 4H-SiC substrate (thickness: $W_{\text{sub}}=300 \mu\text{m}$). The bulk lifetimes in the epilayer and substrate are denoted by τ_{epi} and τ_{sub} , respectively. The bulk lifetime in the substrate (τ_{sub}) was fixed at $0.04 \mu\text{s}$, as experimentally measured. The bulk lifetime of the epilayer (τ_{epi}) was varied in a wide range from 0.1 to $100 \mu\text{s}$. The epilayer thickness (W_{epi}) was changed from 10 to $300 \mu\text{m}$ as another important parameter. The boundary conditions are expressed as follows:

$$D \left. \frac{dp_e}{dx} \right|_{x=0} = s_{r1} p_e, \quad (2)$$

$$D \left. \frac{dp_e}{dx} \right|_{x=W_{\text{epi}}+W_{\text{sub}}} = -s_{r2} p_e, \quad (3)$$

where s_{r1} and s_{r2} are the surface recombination velocities (SRVs) at the epilayer surface and the substrate backside, respectively. Both the SRVs (s_{r1} and s_{r2}) were varied as parameters from 0 to $1 \times 10^6 \text{ cm/s}$. However, the backside recombination velocity (s_{r2}) did not influence the decay curves at all, because the excess carrier concentration at the backside was always many orders-of-magnitude lower than that inside the epilayer, due to the very short lifetime and the large thickness of the substrate. Thus, the backside recombination velocity was assumed to be constant, $1 \times 10^5 \text{ cm/s}$.

Instead, it turned out that the depth profile of excess carriers is greatly influenced by the value of the epilayer-SRV. Hence, the epilayer-SRV (s_{r1}) is called simply the SRV hereafter.

In the present simulation, the typical condition of microwave photoconductance decay (μ -PCD) measurements at room temperature has been assumed. An yttrium lithium fluoride (YLF)-third harmonic generation (3HG) laser ($\lambda = 349 \text{ nm}$) was supposed as an excitation source. The photon density irradiated onto the sample surface was $1 \times 10^{14} \text{ cm}^{-2}$, which leads to a high injection level of mid 10^{15} – 10^{16} cm^{-3} in lightly doped epilayers (typical donor concentration: $1 \times 10^{15} \text{ cm}^{-3}$). Under such high injection condition, the carrier diffusion in the epilayer can be assumed to proceed in an ambipolar mode.³⁰ An ambipolar diffusion constant of $4.2 \text{ cm}^2/\text{s}$ (Ref. 31) was employed for the epilayer, while a standard hole diffusion constant of $0.3 \text{ cm}^2/\text{s}$ was assumed for the substrate, due to the high doping concentration. In real samples, a small potential barrier for holes exists at the epilayer/substrate interface, which originates from the large doping difference. This small potential barrier can repel the holes and suppress the hole diffusion toward the substrate. Under the high injection condition, however, the potential barrier will be reduced by a shielding effect and become less important in the carrier diffusion.

As the initial condition ($t=0$), the depth profile of the hole concentration generated by the YLF-3HG laser was employed. The optical absorption coefficient at the laser wavelength (349 nm) was obtained as 330 cm^{-1} from a literature.³²

III. SIMULATION OF DECAY CURVES

Figure 2 depicts the depth profiles of the excess carrier concentration in a 4H-SiC epilayer on a substrate as a function of time (from $t=0$ to $t=5 \mu\text{s}$, time interval= $0.5 \mu\text{s}$). In this case, the bulk lifetime in the epilayer and the SRV were assumed to be $5.0 \mu\text{s}$ and $1 \times 10^3 \text{ cm/s}$, respectively. The epilayer thickness is (a) $50 \mu\text{m}$ and (b) $200 \mu\text{m}$. Because of the short carrier lifetime in the substrate ($0.04 \mu\text{s}$), the excess carriers generated in the substrate disappear almost completely within the first 0.2 – $0.3 \mu\text{s}$, and the carriers in the epilayer near the epilayer/substrate interface diffuse toward the substrate, due to a large gradient in the carrier concentration. This diffusion enhances fast recombination of generated carriers. For the $50\text{-}\mu\text{m}$ -thick epilayer, a significant portion (about 30% – 35%) of generated carriers is recombined inside the substrate in a short time of $0.5 \mu\text{s}$ after the excitation pulse. Due to a relatively large SRV assumed in the present simulation, about 15% of generated carriers is killed at the surface in the first $0.5 \mu\text{s}$. When the time proceeds, the carrier profile is still severely dominated by recombination at the surface as well as in the substrate, as shown in Fig. 2(a). After $5 \mu\text{s}$, corresponding to the bulk lifetime of the epilayer, about 98% of generated carriers is already lost. In the case of $200\text{-}\mu\text{m}$ -thick epilayer, however, the impact of substrate recombination on the carrier profile is much smaller. Although the fast recombination in the sub-

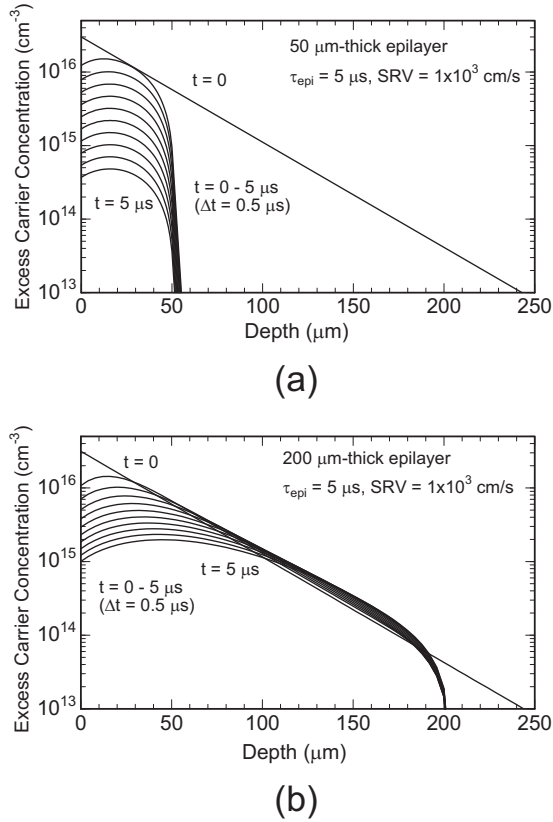


FIG. 2. Depth profiles of the excess carrier concentration in a 4H-SiC epilayer on a substrate as a function of time (from $t=0$ to $t=5 \mu\text{s}$, time interval= $0.5 \mu\text{s}$). In this case, the bulk lifetime in the epilayer was assumed to be $5.0 \mu\text{s}$, and the SRV $1 \times 10^3 \text{ cm/s}$. The epilayer thickness is (a) $50 \mu\text{m}$ and (b) $200 \mu\text{m}$

strate also takes place, the amount of carriers which recombine in the substrate is only 1%–2% of the total generated carriers in the first $0.5 \mu\text{s}$, as shown in Fig. 2(b). The surface recombination gives large influence on the carrier profile when the epilayer is very thick, as expected.

Based on the time-dependent depth profiles of excess carriers, the decay curves were calculated by integrating the excess carrier concentration in 4H-SiC (from $x=0$ to $x=W_{\text{epi}}+W_{\text{sub}}$) as a function of time. Taking account of the microwave frequency (26 GHz) employed in the experiment and the electrical conductivity of SiC after the laser excitation, the depth, to which the μ -PCD measurements monitor, is estimated to be, at least, $200 \mu\text{m}$. In the present numerical simulation, the epilayer thickness (W_{epi}), the bulk lifetime in the epilayer (τ_{epi}), and the SRV were varied in the wide ranges, and the carrier profiles and thereby the simulated decay curves were obtained.

Figure 3 shows the decay curves of excess carrier concentration in 4H-SiC for different SRVs. In this particular case, a carrier lifetime of $5.0 \mu\text{s}$ was used as a bulk lifetime in the (a) $50 \mu\text{m}$ and (b) $200\text{-}\mu\text{m}$ -thick epilayers. All the decay curves are normalized by the integrated carrier concentration at $t=0$. In Fig. 3, a single exponential decay with a lifetime of $5.0 \mu\text{s}$ is plotted by a broken line as a reference.

When the epilayer thickness is $50 \mu\text{m}$ [Fig. 3(a)], the decay curves exhibit fast decay with a much steeper slope

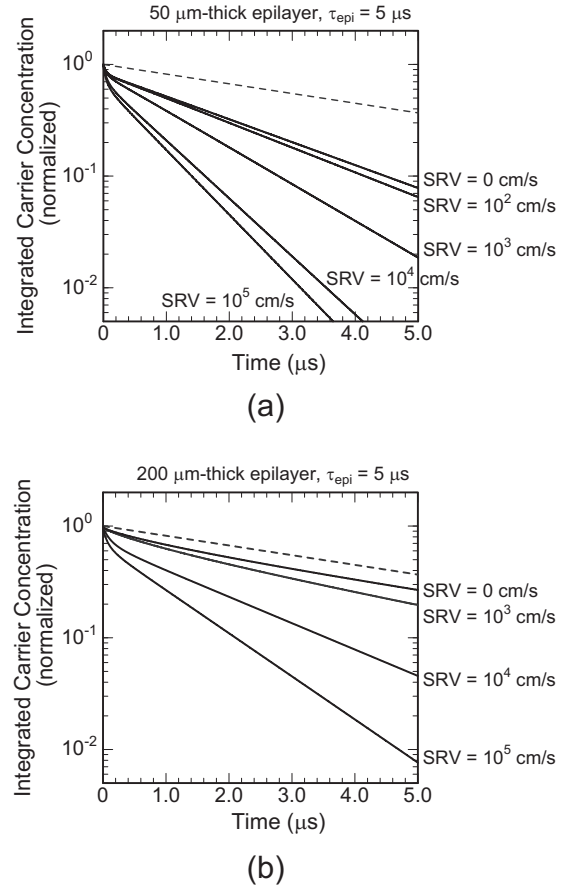


FIG. 3. Decay curves of excess carrier concentration in 4H-SiC for different SRVs. In this case, a carrier lifetime of $5.0 \mu\text{s}$ was used as a bulk lifetime in the (a) $50 \mu\text{m}$ and (b) $200\text{-}\mu\text{m}$ -thick epilayers. A single exponential decay with a lifetime of $5.0 \mu\text{s}$ is plotted by a broken line for a reference.

than the broken line ($5.0 \mu\text{s}$ -exponential curve) at the beginning, even if the SRV is 0 cm/s . Note that the difference between the decay curve for a zero-SRV and the $5.0 \mu\text{s}$ -exponential curve is attributed to the carrier recombination in the substrate. Thus, the impact of recombination in the substrate could be clearly separated from that of surface and bulk recombination. In addition to the substrate recombination, the surface recombination severely affects the decay curves when the SRV is larger than 1000 cm/s . The “effective carrier lifetime,” which was defined from the slope of the main decay curve (after the fast initial decay) simulated in this study, was estimated to be $2.1 \mu\text{s}$, $1.3 \mu\text{s}$, and $0.77 \mu\text{s}$ for SRV of 0 cm/s , 10^3 cm/s , and 10^5 cm/s , respectively. (This effective carrier lifetime corresponds to the lifetime which should be obtained in the actual lifetime measurements.) Although the SRV of 4H-SiC epilayers is not known, it is unlikely that the surface shows a very low recombination velocity ($\sim 100 \text{ cm/s}$). Even in Si, a special surface treatment is required to obtain a sufficiently low SRV ($< 100 \text{ cm/s}$).³³ The situation is much different in the case of very thick epilayers. As shown in Fig. 3(b), the simulated decay curve is close to the $5.0 \mu\text{s}$ -exponential curve (broken line) when the SRV is 0 cm/s , indicating that the substrate recombination gives little influence, as expected from Fig. 2(b). However, the surface recombination governs the effective lifetime, especially when the SRV is larger than

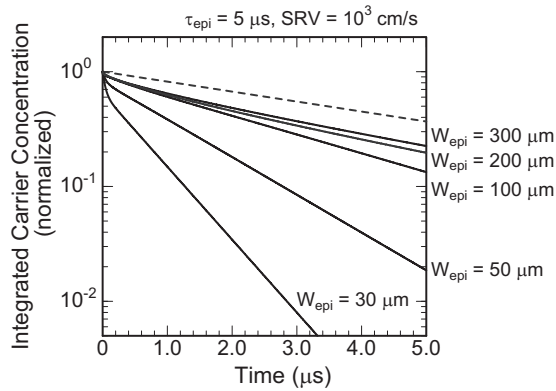


FIG. 4. Decay curves simulated for 30, 50, 100, 200, and 300- μm -thick epilayers. In this simulation, the bulk lifetime of epilayers and the SRV were assumed to be 5.0 μs and 1000 cm/s , respectively. A single exponential curve with a lifetime of 5.0 μs is indicated by a broken line.

10³ cm/s . The effective carrier lifetime was estimated to be 4.8 μs , 4.0 μs , and 1.1 μs for SRV of 0 cm/s , 10³ cm/s , and 10⁵ cm/s , respectively, in the case of the 200- μm -thick epilayer.

The influence of epilayer thickness on the lifetime measurements is highlighted in Fig. 4, where the decay curves simulated for 30, 50, 100, 200, and 300- μm -thick epilayers are presented. In this simulation, the bulk lifetime of epilayers and the SRV were assumed to be 5.0 μs and 1000 cm/s , respectively. Again, a single exponential curve with a lifetime of 5.0 μs is indicated by a broken line in the figure. The effective lifetimes determined from the slope of the simulated decay curves are 0.69, 1.3, 2.7, 4.0, and 4.7 μs for 30, 50, 100, 200, and 300- μm -thick epilayers. Thus, the carrier lifetime will be significantly underestimated when the epilayer thickness is smaller than 100 μm . As shown in Fig. 4, the fast initial decay becomes more pronounced for thinner epilayers, because more portion of generated carriers are lost in the substrate.

Since the carrier lifetimes of n-type 4H-SiC epilayers have been remarkably improved by elimination of the $Z_{1/2}$ center in recent years,^{25–29} much care has to be paid for accurate lifetime measurements. As described above, the measured carrier lifetime can be severely limited by the surface recombination, and the recombination in the substrate can also dominate the measured lifetime when the epilayers are not thick enough. In Sec. IV, the simulated results are compared with experimental results, and the minimum thickness required for accurate lifetime measurements is discussed.

IV. COMPARISON WITH EXPERIMENTAL RESULTS AND DISCUSSION

In experiments, n-type 4H-SiC epilayers were prepared by horizontal hot-wall chemical vapor deposition (CVD) on highly-doped n-type 8° off-axis (0001) substrates.^{34,35} The typical growth temperature and the growth rate were 1650 °C and 24 $\mu\text{m/h}$, respectively. Details of growth process can be found in a previous publication.³⁵ The donor concentration of all the epilayers intentionally doped with nitrogen was in the range from 9×10^{14} to 3×10^{15} cm^{-3} . Deep level transient spectroscopy measurements were per-

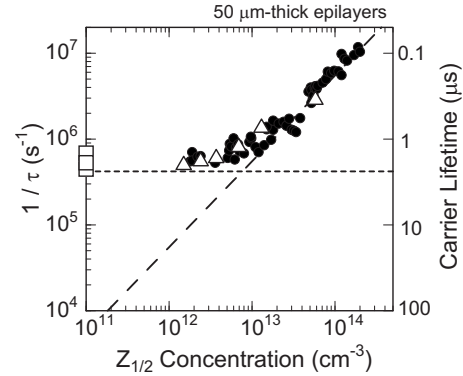


FIG. 5. Inverse of the carrier lifetime vs the concentration of the $Z_{1/2}$ center measured for 50- μm -thick n-type 4H-SiC epilayers. The data denoted by closed circles are the same as those presented in a previous report (Ref. 18). The open triangles indicate the data obtained in latest experiments where the C/Si ratio was changed. The open squares denote the data obtained for the samples in which the $Z_{1/2}$ center was eliminated by the two-step thermal treatment.

formed on Ni/4H-SiC structure in the temperature range from 100 to 760 K. For all the as-grown epilayers investigated in this study, the $Z_{1/2}$ center was the most dominant deep level. For several samples, two-step thermal treatment, namely thermal oxidation at 1300 °C for 5 h followed by Ar annealing at 1550 °C or 30 min was performed in order to eliminate the $Z_{1/2}$ (and EH6/7) center.^{28,29} After this two-step thermal treatment, the $Z_{1/2}$ concentration could be reduced down to below a detection limit (1×10^{11} cm^{-3}). In $\mu\text{-PCD}$ measurements, an YLF-third harmonic generation laser ($\lambda = 349$ nm) was used, where the photon density irradiated onto the sample surface was 1×10^{14} cm^{-2} . The spot size of the excitation laser is approximately 2 mm in diameter. Before the lifetime measurements, samples were cleaned by the RCA process³⁶ followed by HF dipping.

Figure 5 shows the inverse of the carrier lifetime versus the concentration of the $Z_{1/2}$ center measured for 50- μm -thick n-type 4H-SiC epilayers. The data denoted by closed circles are the same as those presented in a previous report.¹⁸ The open triangles indicate the data obtained in latest experiments where the C/Si ratio was changed. By increasing the C/Si ratio from 0.8 to 1.5 during CVD, the $Z_{1/2}$ concentration was reduced from 6.2×10^{13} to 1.5×10^{12} cm^{-3} .³⁷ The open squares denote the data obtained for the samples in which the $Z_{1/2}$ center was eliminated by the two-step thermal treatment. All these data indicate that the carrier lifetimes in 50- μm -thick epilayers are dominated by other recombination paths than the $Z_{1/2}$ center when the $Z_{1/2}$ concentration is lower than about $(1-2) \times 10^{13}$ cm^{-3} . However, this critical concentration must depend on the epilayer thickness (as well as the injection level and temperature), as discussed later.

The effective lifetimes obtained from the simulated decay curves are plotted as a function of the bulk lifetime of the epilayers in Fig. 6. In this simulation, the epilayer thickness was also varied as a parameter, while the SRV was fixed to be 1000 cm/s . As shown in Fig. 6, when the epilayer thickness is 50 μm and the bulk lifetime of an epilayer is shorter than 0.5 μs , the effective lifetime is nearly equal to the bulk lifetime of an epilayer (the effective lifetime is only 4%–

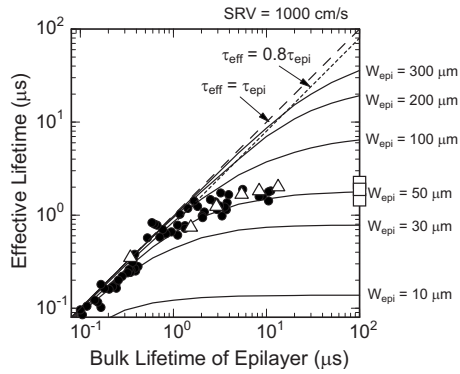


FIG. 6. Effective lifetimes obtained from the simulated decay curves (τ_{eff}) vs the bulk lifetime of the epilayers (τ_{epi}). In this simulation, the epilayer thickness was varied as a parameter, while the SRV was fixed to be 1000 cm/s. The experimental relationship between the measured lifetime and the bulk lifetime obtained from the data shown in Fig. 5 is also plotted. Regarding the experimental data, the same symbols as those in Fig. 5 are used. The dashed and dotted lines indicate $\tau_{\text{eff}} = \tau_{\text{epi}}$ and $\tau_{\text{eff}} = 0.8 \tau_{\text{epi}}$, respectively.

20% shorter). However, the effective lifetime shows saturation at a value of 1.8 μs for 50- μm -thick epilayers when the bulk lifetime exceeds 30 μs . At a 10 μs bulk lifetime, for example, the effective lifetime is only 1.5 μs , indicating almost detrimental underestimation. When the bulk lifetime is long, e.g., 10 μs , the effective lifetime increases with increasing the epilayer thickness, and reaches 8.5 μs for an epilayer thickness of 300 μm . If an extremely long bulk lifetime of 100 μs is achieved, an even thicker epilayer is required for accurate evaluation of carrier lifetimes, unless effective surface passivation is established. On the other hand, it is very hard to obtain accurate bulk lifetimes for 10- μm -thick epilayers, as shown in Fig. 6. These results clearly indicate the impacts of carrier recombination in the substrates on the lifetime measurements. Of course, the absolute values of effective lifetimes shown in Fig. 6 depend on the SRV as well but the trend will be universal.

If the bulk lifetimes of present n-type 4H-SiC epilayers are dominated by a Shockley-Read-Hall (SRH) recombination via the $Z_{1/2}$ center,¹⁵⁻¹⁹ a simple relationship between the bulk lifetime (τ_{epi}) and the $Z_{1/2}$ concentration (N_Z) can be established based on the results in Fig. 5 (broken line) as follows:

$$\tau_{\text{epi}}(\mu\text{s}) = 2 \times 10^{13} / N_Z (\text{cm}^{-3}). \quad (4)$$

Note that this equation is valid when the Auger recombination and recombination at extended defects are less important but it does not depend on the epilayer thickness and the SRV. The factor 2×10^{13} also depends on the excitation intensity (injection level) and temperature. Using this equation, the bulk lifetimes in epilayers were estimated from the $Z_{1/2}$ concentration. Thus, the experimental relationship between the measured lifetime and the bulk lifetime was obtained from the data shown in Fig. 5. This relationship is plotted in Fig. 6, considering that the measured lifetime corresponds to the effective lifetime in the simulation. Regarding the experimental data, the same symbols as in Fig. 5 are used. (It is not easy to estimate the bulk lifetime for the samples in which the $Z_{1/2}$ center was eliminated, denoted by the open squares, because other defects must limit the bulk lifetimes. In this

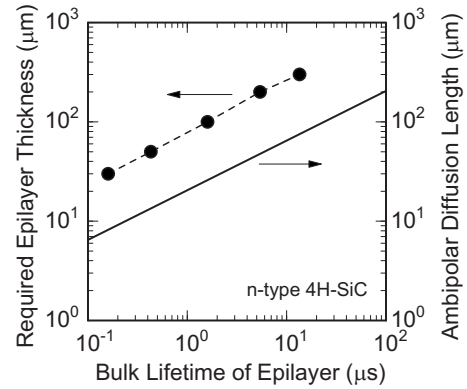


FIG. 7. Epilayer thickness required for obtaining 80% of bulk lifetime in the measurement ($\tau_{\text{eff}} = 0.8 \tau_{\text{epi}}$) as a function of the bulk lifetime. The SRV was assumed to be 1000 cm/s. The ambipolar diffusion length, which was calculated by using an ambipolar diffusion constant of 4.2 cm^2/s , (Ref. 31) is also shown.

study, however, the lifetime estimated from Eq. (4) are plotted for simplicity.)

It is natural that the effective lifetime is nearly equal to the bulk lifetime when the bulk lifetime is short, less than 1 μs because the lifetime is indeed limited by the $Z_{1/2}$ center in this region. The effective lifetimes tend to saturate at about 2 μs when the bulk lifetime is very long, being in good agreement with the result simulated for 50- μm -thick epilayers, as shown in Fig. 6. Thus, the other recombination paths, which limit the measured lifetimes in 4H-SiC epilayers with low $Z_{1/2}$ concentrations as indicated by a dotted line in Fig. 5, may be mainly the surface recombination and fast recombination in the substrate. For more quantitative comparison between the experimental and simulated results, the SRV of SiC must be experimentally determined.

From Fig. 6, one can estimate the minimum epilayer thickness required for accurate lifetime measurements. Since the measured lifetimes are always underestimated, it is assumed that 20% underestimation is acceptable in this study. The minimum epilayer thickness to obtain 80% of a bulk lifetime ($0.8 \tau_{\text{epi}}$) can be estimated from the cross point between 80% line of the bulk lifetime (dotted line: $\tau_{\text{eff}} = 0.8 \tau_{\text{epi}}$) and a simulated curve (solid line). The epilayer thickness required for obtaining 80% of a bulk lifetime in the measurement is plotted by closed circles in Fig. 7 as a function of the bulk lifetime. The required epilayer thickness is 50 μm for a bulk lifetime of 0.43 and 300 μm for 13.5 μs , if the SRV is 1000 cm/s. In the figure, the ambipolar diffusion length, which was calculated by using an ambipolar diffusion constant of 4.2 cm^2/s ,³¹ is also shown. It is of interest that the minimum epilayer thickness required for lifetime measurements is approximately four times larger than the ambipolar diffusion length at any bulk lifetime. Note that the required epilayer thickness slightly decreases if the SRV is decreased, and vice versa.

Since it is revealed that the recombination in a substrate greatly affects the lifetime measurements, epilayers with different thicknesses were prepared to experimentally investigate the influence of substrate recombination. n-type 4H-SiC epilayers with a thickness of 50, 98, and 148 μm were grown on highly-doped substrates. The donor concentration

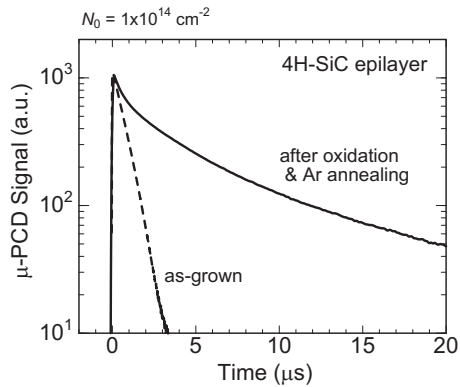


FIG. 8. μ -PCD decay curves at room temperature obtained from a 148- μm -thick n-type 4H-SiC epilayer before (as-grown) and after the two-step thermal treatment. The photon density irradiated onto the sample surface was $1 \times 10^{14} \text{ cm}^{-2}$.

of the epilayers was $(0.9-1) \times 10^{15} \text{ cm}^{-3}$. After the lifetime measurements on as-grown materials by a μ -PCD method, two-step thermal treatment, thermal oxidation at 1300 °C for 5 h followed by Ar annealing at 1550 °C for 30 min was performed in order to eliminate the $Z_{1/2}$ (and EH6/7) center.^{28,29} Note that the thermal oxides were removed before Ar annealing. After this defect reduction process, the lifetime measurements were repeated. Figure 8 shows the μ -PCD decay curves at room temperature obtained from a 148- μm -thick epilayer before (as-grown) and after the two-step thermal treatment. The photon density irradiated onto the sample surface was $1 \times 10^{14} \text{ cm}^{-2}$. For the as-grown epilayer, the measured lifetime is 0.69 μs , while the lifetime is remarkably improved to 9.5 μs after the thermal treatment owing to significant reduction in the $Z_{1/2}$ center.

The dependence of measured lifetimes on the epilayer thickness is presented in Fig. 9, where the lifetimes before and after the two-step thermal treatment are plotted by closed and open circles, respectively. In the figure, the simulated dependence of the lifetime on the epilayer thickness is also shown by dashed lines, for various bulk lifetimes of epilayers. In the simulation, the SRV was again assumed to be 1000 cm/s. For as-grown epilayers, the measured lifetimes were almost independent of the epilayer thickness in the investigated range,

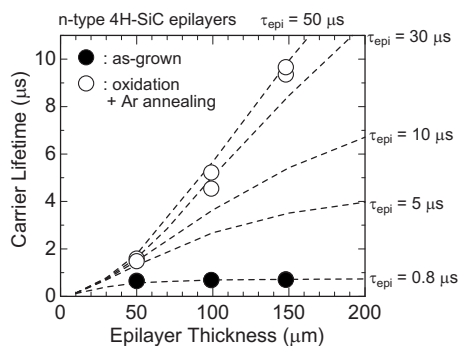


FIG. 9. Dependence of measured lifetimes on the epilayer thickness, where the lifetimes before and after the two-step thermal treatment are plotted by closed and open circles, respectively. The simulated dependence of lifetimes on the epilayer thickness is also shown by dashed lines, for various bulk lifetimes of epilayers. In the simulation, the surface recombination was again assumed to be 1000 cm/s.

and showed good agreement with the result simulated for a bulk lifetime of 0.8 μs . In the as-grown epilayers, SRH recombination via the $Z_{1/2}$ center is dominant, and the impact of carrier recombination in substrates is less important. In contrast, the measured lifetimes exhibit significant increase with increasing the epilayer thickness for samples with greatly reduced $Z_{1/2}$ concentration, suggesting that the dominant recombination path is changed from the SRH recombination to the recombination in the substrates for high-quality epilayers. Although it is difficult to estimate the real bulk lifetime in the epilayers after the two-step thermal treatment due to the lack of experimental SRV values, the bulk lifetime may be about 30 μs or even longer, as seen from Fig. 9.

V. CONCLUSION

Impacts of carrier recombination at the epilayer-surface as well as in the substrate on carrier lifetimes in 4H-SiC epilayers were investigated by using numerical simulation based on a diffusion equation. The simulation revealed that the fast carrier recombination in the substrate severely affects the decay curves when the bulk lifetime is relatively long and the epilayer is not thick enough. The surface recombination also causes underestimation of carrier lifetimes, especially when the SRV is larger than 10^3 cm/s . The fast decay often observed at the initial stage of decay curves can be explained by fast recombination at the surface and in the substrate. For accurate measurement of carrier lifetimes, a very thick ($>100 \mu\text{m}$) epilayer is required if the bulk lifetime in the epilayer is longer than several microsecond. The minimum epilayer thickness required for accurate lifetime measurements was estimated as about four times of the ambipolar diffusion length. In experimental study on a 148- μm -thick n-type epilayer, the carrier lifetime was improved from 0.69 to 9.5 μs by reducing the $Z_{1/2}$ center via two-step thermal treatment, thermal oxidation at 1300 °C for 5 h and Ar annealing at 1550 °C for 30 min. The real bulk lifetime may be about 30 μs or even longer, as judged from comparison with simulated results. Regarding the influence of extended defects on carrier lifetime, however, further investigation is required.

ACKNOWLEDGMENTS

This work was supported by the Funding Program for World-Leading Innovative R&D on Science and Technology (FIRST Program), a Grant-in-Aid for Scientific Research (Grant No. 21226008) from the Japan Society for the Promotion of Science, and the Global COE Program (C09) from the Ministry of Education, Culture, Sports, and Technology, Japan.

¹H. Matsunami and T. Kimoto, *Mater. Sci. Eng. R.* **20**, 125 (1997).

²J. A. Cooper, Jr., M. R. Melloch, R. Singh, A. Agarwal, and J. W. Palmour, *IEEE Trans. Electron Devices* **49**, 658 (2002).

³R. Rupp, M. Treu, A. Mauder, E. Griebel, W. Werner, W. Bartsch, and D. Stephani, *Mater. Sci. Forum* **338-342**, 1167 (2000).

⁴P. Friedrichs, H. Mitlehner, R. Kaltschmidt, U. Weinert, W. Bartsch, C. Hecht, K. O. Dohnke, B. Weis, and D. Stephani, *Mater. Sci. Forum* **338-342**, 1243 (2000).

⁵H. Lendenmann, F. Dahlquist, J. P. Bergman, H. Bleichner, and C. Hallin, *Mater. Sci. Forum* **389-393**, 1259 (2002).

- ⁶Y. Sugawara, D. Takayama, K. Asano, A. Agarwal, S. Ryu, J. Palmour, and S. Ogata, Proceedings of International Symposium on Power Semiconductor Devices and ICs, 24–27 May 2004, Kitakyusyu (IEE of Japan, Tokyo, 2004), p. 365.
- ⁷J. Wang, A. Q. Huang, W. Sung, Y. Liu, and B. J. Baliga, *IEEE Industrial Electronics Magazine* (IEEE, New York, 2009), p. 16.
- ⁸J. P. Bergman, O. Kordina, and E. Janzén, *Phys. Status Solidi A* **162**, 65 (1997).
- ⁹L. Storasta, J. P. Bergman, C. Hallin, and E. Janzén, *Mater. Sci. Forum* **389–393**, 549 (2002).
- ¹⁰J. P. Bergman, H. Jakobsson, L. Storasta, F. H. C. Carlsson, B. Magnusson, S. Sridhara, G. Pozina, H. Lendenmann, and E. Janzén, *Mater. Sci. Forum* **389–393**, 9 (2002).
- ¹¹J. Zhang, L. Storasta, J. P. Bergman, N. T. Son, and E. Janzén, *J. Appl. Phys.* **93**, 4708 (2003).
- ¹²T. Dalibor, G. Pensl, H. Matsunami, T. Kimoto, W. J. Choyke, A. Schöner, and N. Nordell, *Phys. Status Solidi A* **162**, 199 (1997).
- ¹³C. Hemmingsson, N. T. Son, O. Kordina, J. P. Bergman, E. Janzén, J. L. Lindström, S. Savage, and N. Nordell, *J. Appl. Phys.* **81**, 6155 (1997).
- ¹⁴T. Tawara, H. Tsuchida, S. Izumi, I. Kamata, and K. Izumi, *Mater. Sci. Forum* **457–460**, 565 (2004).
- ¹⁵P. B. Klein, B. V. Shanabrook, S. W. Huh, A. Y. Polyakov, M. Skowronski, J. J. Sumakeris, and M. J. O’Loughlin, *Appl. Phys. Lett.* **88**, 052110 (2006).
- ¹⁶K. Danno, D. Nakamura, and T. Kimoto, *Appl. Phys. Lett.* **90**, 202109 (2007).
- ¹⁷P. B. Klein, *J. Appl. Phys.* **103**, 033702 (2008).
- ¹⁸T. Kimoto, K. Danno, and J. Suda, *Phys. Status Solidi B* **245**, 1327 (2008).
- ¹⁹S. A. Reshanov, W. Bartsch, B. Zippelius, and G. Pensl, *Mater. Sci. Forum* **615–617**, 699 (2009).
- ²⁰L. Storasta, J. P. Bergman, E. Janzén, A. Henry, and J. Lu, *J. Appl. Phys.* **96**, 4909 (2004).
- ²¹I. Pintilie, U. Grossner, B. G. Svensson, K. Irmschner, and B. Thomas, *Appl. Phys. Lett.* **90**, 062113 (2007).
- ²²K. Danno and T. Kimoto, *J. Appl. Phys.* **100**, 113728 (2006).
- ²³S. I. Maximenko, J. A. Freitas, Jr., P. B. Klein, A. Shrivastava, and T. S. Sudarshan, *Appl. Phys. Lett.* **94**, 092101 (2009).
- ²⁴J. Hassan and J. P. Bergman, *J. Appl. Phys.* **105**, 123518 (2009).
- ²⁵L. Storasta and H. Tsuchida, *Appl. Phys. Lett.* **90**, 062116 (2007).
- ²⁶L. Storasta, H. Tsuchida, T. Miyazawa, and T. Ohshima, *J. Appl. Phys.* **103**, 013705 (2008).
- ²⁷H. Tsuchida, M. Ito, I. Kamata, M. Nagano, T. Miyazawa, and N. Hoshino, *Mater. Sci. Forum* **645–648**, 77 (2010).
- ²⁸T. Hiyoshi and T. Kimoto, *Appl. Phys. Express* **2**, 041101 (2009).
- ²⁹T. Hiyoshi and T. Kimoto, *Appl. Phys. Express* **2**, 091101 (2009).
- ³⁰S. M. Sze, *Physics of Semiconductor Devices*, 2nd ed. (Wiley, New York, 1981), Chap. 2.
- ³¹P. Grivickas, J. Linnros, and V. Grivickas, *J. Mater. Res.* **16**, 524 (2001).
- ³²S. G. Sridhara, R. P. Devaty, and W. J. Choyke, *J. Appl. Phys.* **84**, 2963 (1998).
- ³³D. K. Schroder, *Semiconductor Materials and Device Characterization*, 3rd ed. (Wiley, New York, 2006), Chap. 7.
- ³⁴T. Kimoto, S. Nakazawa, K. Hashimoto, and H. Matsunami, *Appl. Phys. Lett.* **79**, 2761 (2001).
- ³⁵T. Hori, K. Danno, and T. Kimoto, *J. Cryst. Growth* **306**, 297 (2007).
- ³⁶W. Kern and D. A. Puotinen, *RCA Rev.* **31**, 187 (1970).
- ³⁷T. Kimoto, K. Hashimoto, and H. Matsunami, *Jpn. J. Appl. Phys., Part 1* **42**, 7294 (2003).